Theoretical study of the effect of local flow disturbances on the concentration of low-density lipoproteins at the luminal surface of end-to-end anastomosed vessels

S. Wada[1] **M. Koujiya**[2] **T. Karino**[1]

[1]Research Institute for Electronic Science, Hokkaido University, Sapporo, Japan
[2]R&D Center, Nikkiso Co., Ltd, Shizuoka, Japan

Abstract—*To elucidate the mechanisms of localisation of intimal hyperplasia in anastomosed arteries, the effects of flow disturbances on the transport of low-density lipoproteins (LDLs) from the flowing blood to the wall of end-to-end anastomosed arteries, with and without a moderate stenosis, were studied theoretically by means of a computer simulation under the condition of steady flow. In an artery with moderate stenosis at the anastomotic junction and intimal thickening distal to it, we found that, owing to the water-permeable nature of the arterial wall, the surface concentration of LDL was elevated up to 20% higher than that of the bulk flow distal to the stenosis, where a recirculation zone was formed and wall shear stresses were low. In contrast to this, no significant elevation of surface concentration of LDLs occurred in another anastomosed vessel in which no stenosis was formed and no intimal thickening was observed. These results suggest that flow-dependent concentration polarisation of LDLs plays a causative role in the localisation of anastomotic intimal hyperplasia in the human arterial system by locally elevating the surface concentration of LDLs, thus augmenting their uptake by endothelial cells.*

Keywords—*Anastomosis, Intimal hyperplasia, Mass transfer, Blood flow, Concentration polarisation, Low-density lipoprotein*

Med. Biol. Eng. Comput., 2002, **40**, 576–587

1 Introduction

INTIMAL HYPERPLASIA at the anastomotic junction of a host artery and a synthetic or an autologous vein graft is a major cause of late failure in vascular reconstruction (IMPARATO *et al.*, 1972). Despite the development of several biocompatible synthetic grafts, such as polytetrafluoroethylene grafts (GUIDOIN et at., 1988), and improvement of operative techniques by incorporating a vein cuff or a patch in end-to-side anastomosis (MILLER *et al.*, 1984; TYRRELL and WOLFE, 1991; TAYLOR *et al.*, 1992), long-term patency of small-diameter grafts is still poor. One of the reasons for that is that the precise mechanisms for the pathogenesis and localisation of intimal hyperplasia have not been elucidated yet.

Anastomotic intimal hyperplasia is caused by invasion and proliferation of smooth muscle cells, fibroblasts and matrix materials derived from the cut end of the host artery (CLOWES *et al.*, 1985). It has been shown that local disturbance of blood flow, which creates a region of low wall shear stress at the anastomotic junction, is related to the localised genesis and development of intimal hyperplasia (SOTTIURAI *et al.*, 1989; BASSIOUNY *et al.*, 1992; ISHIBASHI *et al.*, 1995), and an increase in plasma cholesterol concentration accelerates the disease (KLYACHKIN *et al.*, 1993; BAUMANN *et al.*, 1994).

The process and the appearance of late-stage anastomotic intimal hyperplasia well resemble those of atherosclerosis, in which atherogenic lipoproteins, namely low-density lipoproteins (LDLs), play an important role (ROSS and HARKER, 1976; HOFF and WAGNER, 1986; STARY *et al.*, 1994). In fact, it has been shown that, after coronary artery bypass surgery, atherosclerosis progresses both in the native circulation and the implanted saphenous vein bypass graft, and lowering the lipoprotein level prevents the progression of atherosclerosis (HUNNINGHAKE, 1998; CAMPEAU, 2000).

This suggests that fluid mechanical factors are playing an important role in the pathogenesis and localisation of the vascular diseases by affecting the transport of lipoproteins from flowing blood to the vessel wall. Therefore we have been carrying out theoretical (DENG *et al.*, 1995; WADA and KARINO, 1999; 2002*a*;*b*) and experimental (NAIKI *et al.*, 1999; WADA *et al.*, 2001*a*;*b*) studies on the transport of lipoproteins in blood flowing through arteries of various shapes to their vessel wall, where a monolayer of endothelial cells acts as a barrier to stop macromolecules, such as LDLs, infiltrating the subendothelial space.

Correspondence should be addressed to Dr Shigeo Wada; email: wada@bfd.es.hokudai.ac.jp

Paper received 21 January 2002 and in final form 17 May 2002
MBEC online number: 20023707

The results obtained so far for the cases of a straight portion (WADA and KARINO, 1999) and a curved segment (WADA and KARINO, 2002*a*) of an artery showed that, owing to the semipermeable nature of an arterial wall to plasma, accumulation of lipoproteins occurs at a blood–endothelium boundary, and the concentration of lipoproteins at the luminal surface of the vessel wall varies from place to place as a function of wall shear rate, water filtration velocity at the vessel wall and diffusivity of lipoproteins, resulting in an uneven distribution of LDL concentration at the luminal surface of the vessel wall, which may determine the number of LDLs to be transported from blood to the vessel wall.

The present study was designed to investigate the effect of locally disturbed flows on the distribution of surface concentration of LDLs in end-to-end anastomosed vessels that were used previously by ISHIBASHI *et al.* (1995) to investigate the relationship between flow patterns and precise locations of intimal thickening. To do that, we constructed two anatomically realistic models from the photographs of transparent anastomosed arteries, with and without a moderate stenosis, and carried out computer simulations of blood flow and LDL transport in these arteries.

2 Theoretical modelling and analyses

2.1 *Anatomical model for computation*

The shapes of the blood vessel used in the present study were obtained from tracings of dog femoral arteries containing an end-to-end anastomosis that were harvested 3 months after an operation and rendered transparent using a technique developed by KARINO and MOTOMIYA (1983). We prepared two computational models from the arteries that were cut and anastomosed at a 45° angle and were used in flow studies by ISHIBASHI *et al.* (1995). Fig. 1 shows the shape and thickness of the wall of the anastomosed vessels and detailed flow patterns observed in them in steady flow. It has been shown that, in one of the arteries that contained a moderate stenosis on the inferior wall, a recirculation zone was formed distal to the stenosis, and intimal thickening occurred there (Fig. 1*a*). In the other artery, which was anastomosed smoothly without a stenosis being created, no recirculation zone was formed, and no intimal thickening developed in it (Fig. 1*b*).

Fig. 2 shows the process of constructing an anatomically realistic model for computer simulation. Owing to the lack of detailed data on the geometry of the cross-section of the anastomosed vessel, it was assumed that the vessel was symmetric with respect to its bisector plane, so that the geometry of the cross-section could be expressed by the combination of a semicircle for the upper half of the vessel, where no intimal thickening occurred, and a semi-ellipse for the lower half of the vessel, where intimal thickening occurred.

First of all, the outlines of the vessel, obtained by tracing the outlines of both the inner and outer walls of the transparent artery (see Fig. 2*a*), were smoothed by means of a moving average method. Next, the central axis of the vessel was determined by the drawing of 130 lines, at certain intervals along the whole length of the vessel, each of which gave the shortest distance between the two outlines of the outer wall of the vessel, and the drawing of a curved line that connected the midpoint C_i of each of the lines P_iQ_i (see Fig. 2*b*). Furthermore, through each midpoint, a line normal to the central axis of the vessel was drawn between the two outlines of the inner wall of the vessel, and it was defined as the diameter of the vessel at that axial location (see Fig. 2*c*).

The distances from the midpoint to the upper wall (segment C_iq_i) and to the lower wall (segment C_ip_i) were, respectively, assigned to the radius of the semicircle r_{u_i} and a half of the short

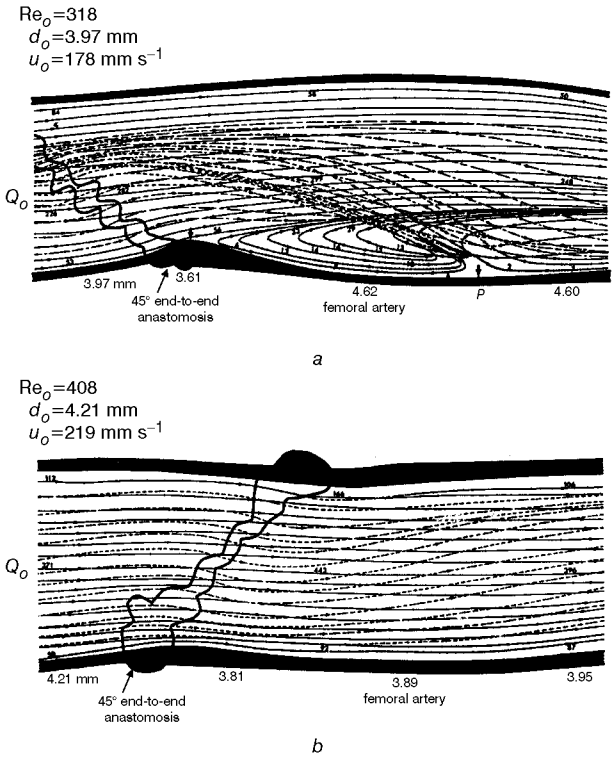

Fig. 1 *Tracings of 45° cut and end-to-end anastomosed dog femoral arteries from which computational models of anastomosed vessels used in present study were constructed, showing shape and thickness of vessel walls and detailed flow patterns observed in vessel under condition of steady flow (adopted and modified from ISHIBASHI et al. (1995) by permission). (a) Anastomosed artery containing moderate stenosis and intimal thickening on inferior wall. (b) Anastomosed artery containing neither stenosis nor intimal thickening*

axis of the semi-ellipse r_{l_i} forming the cross-section of the anastomosed vessel. The segment C_iq_i was also assigned to a half of the long axis of the semi-ellipse r_{z_i}, which was equal to r_{u_i}. The axial lengths of the vessel obtained from the diagram shown in Figs 1*a* and *b* were 17.7 and 16.7 mm, and the diameters at the inlet d_o, where $r_{l_o} = r_{u_o} = d_o/2$, were 3.97 and 4.21 mm, respectively.

To construct a computational mesh model of the blood vessel, a Cartesian co-ordinate (x, y, z) was laid down at the very inlet of the vessel, with its origin located at the centre of the cross-section and the x-, y- and z-axes lying, respectively, on the central axis of the vessel, the bisector plane and the diametrical plane normal to the bisector plane. In each cross-section, an independent local co-ordinate system (y', z') was laid with its origin located at the midpoint C_i and the y'- and z'-axes lying along the segment C_iq_i in the bisector plane and in a plane normal to the bisector plane, respectively.

Then, a circle having a unit length of radius, the centre of which was located at the origin of the local co-ordinate system, was prepared (see Fig. 2*d*). In the circumferential direction, the region greater than $0.5R$ (R = radius of the vessel) was divided into 120 uniform-sized segments. In the radial direction, the region between $0.5R$ and $0.7R$ was divided into five uniform-sized segments, and the region greater than $0.7R$ was divided into 15 segments of gradually diminishing size, which ranged from $0.0497R$ to $0.00497R$ (approximately 10 μm). The region smaller than $0.5R$ was automatically divided into 748 rectangular elements using a mesh-generator in flow-simulation software*. After that, all the positions of the nodal points

*Ansys-Flotran version 5.5, distributed by Cybernet System Co., Japan

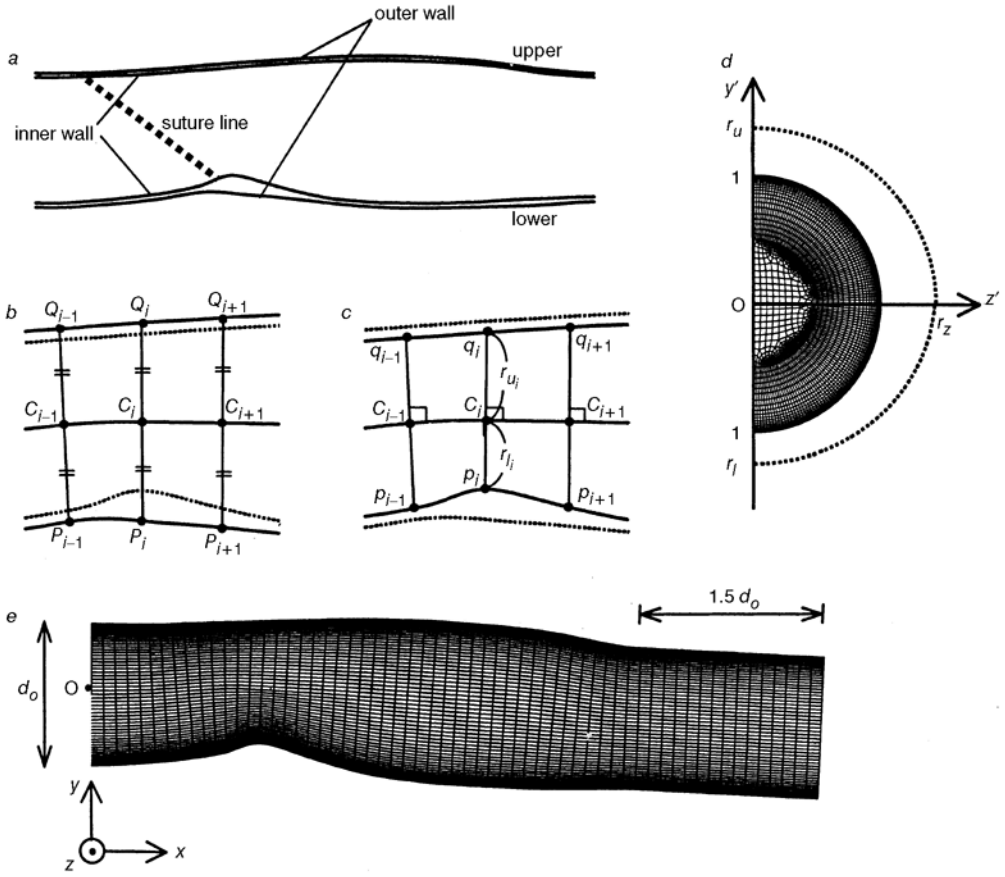

Fig. 2 *Schematic representation of process of constructing anatomically realistic model for computer simulation from tracing of arterial wall, as observed from direction normal to its bisector plane. (a) shape of arterial segment obtained by tracing outlines of both inner and outer walls of transparent artery. (b) Central axis of vessel determined from outer walls. (c) Definition of vessel diameter, radius of upper semicircle r_{u_i} and half of short axis of semi-ellipse r_{l_i} forming cross-section of vessel. (d) Unit circle that was divided into finite elements and put on each cross-section. (e) Three-dimensional mesh model of vessel used in computational analyses*

(y_s', z_s'), constituting the elements within the unit circle, were moved to new nodal positions (y_n', z_n'), using the following formulas, so that the outline of the unit circle coincided with that of the cross-section of the vessel:

$$z_n' = r_z z_s', \quad y_n' = \begin{cases} r_u y_s' & \text{for } y_s' \geq 0 \\ r_l y_s' & \text{for } y_s' < 0 \end{cases} \tag{1}$$

Finally, a mesh model for computations was obtained by arranging the cross-sections divided into finite elements along the vessel and creating hexahedral elements with eight nodes in sequence (see Fig. 2*e*). At this time, the local co-ordinate (y', z') was converted to the global co-ordinate (x, y, z) using the following formulas:

$$\begin{aligned} x &= y' \sin\theta + x_c \\ y &= y' \cos\theta + y_c \\ z &= z' + z_c \end{aligned} \tag{2}$$

where (x_c, y_c, z_c) denotes the location of the midpoint C_i, and θ is the angle between the y-axis and the y'-axis, respectively. To eliminate the end-effect of the boundary at the distal portion of the vessel, the blood vessel was extended distally by adding a straight cylindrical tube with a length of $1.5\,d_o$. The total number of nodes and elements used for the mesh model were 391 919 and 377 760, respectively.

2.2 *Analysis of blood flow*

It was assumed that an arterial wall is rigid and blood is an incompressible Newtonian fluid with a viscosity $\mu = 3.5$ mPa · s and a density $\rho = 1.05 \times 10^3$ kg m^{-3}. Under these assumptions, a steady flow of blood can be described by the continuity and Navier-Stokes equations, as follows:

$$\nabla \cdot \boldsymbol{v} = 0 \tag{3}$$

$$\rho(\boldsymbol{v} \cdot \nabla)\boldsymbol{v} = -\nabla P + \mu \nabla^2 \boldsymbol{v} \tag{4}$$

where $\boldsymbol{v}$ is a velocity vector consisting of three components, namely u, v, w for the x-, y- and z-directions, P is blood pressure, and ρ and μ are the density and the viscosity of blood, respectively.

Boundary conditions applied were: a parabolic velocity profile at the inlet that was determined from the Reynolds number given at the inlet of the artery Re_o; constant pressures at the outlet; axisymmetric conditions for all the variables on the bisector plane; and a non-slip condition at the vessel wall. In the calculation of blood flow, it was assumed that the filtration flow of water at the vessel wall does not affect the flow field.

2.3 *Analysis of mass transport*

Under the assumption that LDL molecules in flowing blood are transported by both diffusion and convection, steady-state mass transport of LDLs can be described by

$$\boldsymbol{v} \cdot \nabla C - D\nabla^2 C = 0 \tag{5}$$

where C is the concentration of LDLs, and D is the diffusivity of LDLs. Using a Stokes–Einstein equation, the diffusivity of LDLs was estimated to be 5.0×10^{-6} mm^2 s^{-1} in blood at a body temperature of 37°C. The velocity vector $\boldsymbol{v}$ was obtained by solving (3) and (4), which govern blood flow.

Boundary conditions applied were a uniform and constant concentration of LDLs at the inlet, zero gradient of LDL concentration in the longitudinal direction at the outlet, an axisymmetric condition with respect to LDL concentration on the bisector plane, and conservation of mass for the LDLs entering the vessel wall, moving towards the vessel wall by a filtration flow and diffusing back to the mainstream, at the vessel wall, as described by

$$V_w C_w - D\left.\frac{\partial C}{\partial \boldsymbol{n}}\right|_{wall} = KC_w \tag{6}$$

where V_w is the filtration velocity of water at the vessel wall, C_w is the concentration of LDLs at the luminal surface of the vessel (surface concentration), $\partial/\partial \boldsymbol{n}$ denotes the differential in the direction normal to the vessel wall, and K is the overall mass transfer coefficient of LDLs at the vessel wall.

In the actual calculations, the values generally reported in the literature as a filtration velocity of water and an overall mass transfer coefficient of LDLs at an arterial wall, 4×10^{-5} mm s^{-1} (TEDGUI and LEVER, 1984) and 2×10^{-7} mm s^{-1} (BRATZLER *et al.*, 1977; TRUSKEY *et al.*, 1992), respectively, were used as representative values for V_w and K under physiological conditions.

2.4 *Procedures for computation*

Numerical solutions for blood pressure and velocity were obtained from (3) and (4) using heat and flow simulation software†, and then various haemodynamic properties, such as velocity profiles, paths of fluid elements and wall shear stresses, were evaluated as follows.

The trajectories of fluid elements in the arterial segment were obtained by integration of the velocity of fluid elements with respect to time, that is, by evaluation of the position vector of a target fluid element $\boldsymbol{r}(t)$, at each time $t(0<t<T)$, using the following formula:

$$\boldsymbol{r}(t+\Delta t) = \boldsymbol{r}(t) + \boldsymbol{v}(\boldsymbol{r})\Delta t \tag{7}$$

where Δt denotes the time step of the evaluation. To ensure the accuracy of the results, calculations were carried out under the following constraint conditions:

$$|\Delta \boldsymbol{r}| = |\boldsymbol{r}(t+\Delta t) - \boldsymbol{r}(t)| \leq 0.001 r_o \tag{8}$$

and

$$\Delta t \leq \frac{0.001 r_o}{u_o} \tag{9}$$

Wall shear stress was evaluated at each node on the vessel wall by calculation of the velocity gradient in the direction normal to the vessel wall, from velocity vectors parallel to the wall at the nodes that constituted the element closest to the vessel wall and by multiplication of it by the viscosity of blood.

Using the fluid velocities obtained at all the nodal points, the governing equation of LDL transport in flowing blood was also numerically solved by employing an in-house program code based on the Galerkin finite element method with a streamline-upwind technique (BROOKS and HUGHES, 1982). In the calculation of mass transfer, the solution domain was limited to the region greater than $0.7R$ at all locations, as concentration polarisation of lipoproteins was expected to occur only within a thin fluid layer adjacent to the vessel wall whose thickness was less than $0.05R$. A constant concentration C_o, which was the same value as that given at the inlet, was applied to the inner boundary of the selected region. Furthermore, to obtain a stable numerical solution with the desired accuracy, the element in the selected region was divided into two sub-elements in the radial directions. The fluid velocity at the newly created node was obtained by carrying out a linear interpolation.

†Star LT version 2.1, distributed by CD Adapco, Japan

3 Results

3.1 *Characteristics of the flow through anastomosed arteries*

Fig. 3 shows the detailed flow pattern and distributions of fluid velocity that were obtained by carrying out calculations of blood flow based on a computational model that was constructed from the shape of an anastomosed artery containing a moderate stenosis, shown in Fig. 1*a*. In this calculation, the Reynolds number at the inlet Re_o was assumed to be 318, which was the same as that used in the flow experiments carried out by ISHIBASHI *et al.* (1995).

The detailed flow pattern shown in Fig. 3*a* was obtained by tracing the paths of fluid elements that were chosen to depict the characteristics of the flow in this vessel. The paths were described using several different types of line, depending on the magnitude of velocity at each location. It was found that owing to the presence of a moderate stenosis on the inferior wall of the vessel, flow separation occurred at location S, around the apex of the stenosis, and then peripheral secondary flows from the anterior and posterior walls entered the region of separated flow from both sides. The fluid elements forming part of the secondary flows slowly moved backwards along the inferior wall on approaching the bisector plane, and then they suddenly changed their directions and were drawn along by the rapid mainstream in and very close to the bisector plane, after describing a single orbit. By comparing the results with the experimentally obtained ones shown in Fig. 1*a*, it was found that the flow pattern obtained by the present computation was qualitatively the same as that found experimentally, although the length of the recirculation zone in the bisector plane (the distance from the separation point S to the stagnation point P) obtained by the simulation was shorter than that obtained experimentally (5.2 mm against 6.7 mm).

Fig. 3*b* shows the distributions of fluid velocity in the bisector plane of the anastomosed artery. Numbers outside the vessel and along the velocity distributions indicate the value of wall shear stress calculated at the location in the bisector plane and the maximum values in the velocity distribution, respectively. Vector plots of a flow pattern and a contour map of the fluid axial velocity in the cross-section of the vessel are also shown in the Figure, respectively, in the right and left halves of the cross-section at each location where a velocity distribution is shown. It was found that the direction of the secondary flow changed at the apex of the stenosis, and then the peripheral flow headed to the inferior wall at sites distal to the stenosis. It was also found that the distribution of axial velocity was largely affected by the presence of the stenosis, which created regions of high wall shear stress around the apex of the stenosis and low wall shear stress at the inferior wall of the vessel distal to the stenosis, where anastomotic intimal thickening developed.

Figs 4*a* and *b* show the results of the calculation of blood flow at $Re_o = 408$ for the anastomosed artery containing no stenosis shown in Fig. 1*b*. As shown in these Figures, it was found that the fluid elements in the main flow passed through the artery almost parallel to the vessel wall, as shown by the solid lines in Fig. 4*a*, and velocity profiles remained quasi-parabolic throughout the entire arterial segment, as shown in Fig. 4*b*. Because of a slight constriction of the vessel at the site of anastomosis, the slow peripheral flows adjacent to the anterior and posterior walls were slightly disturbed at the anastomotic junction, as can be seen by the wavy paths of fluid elements

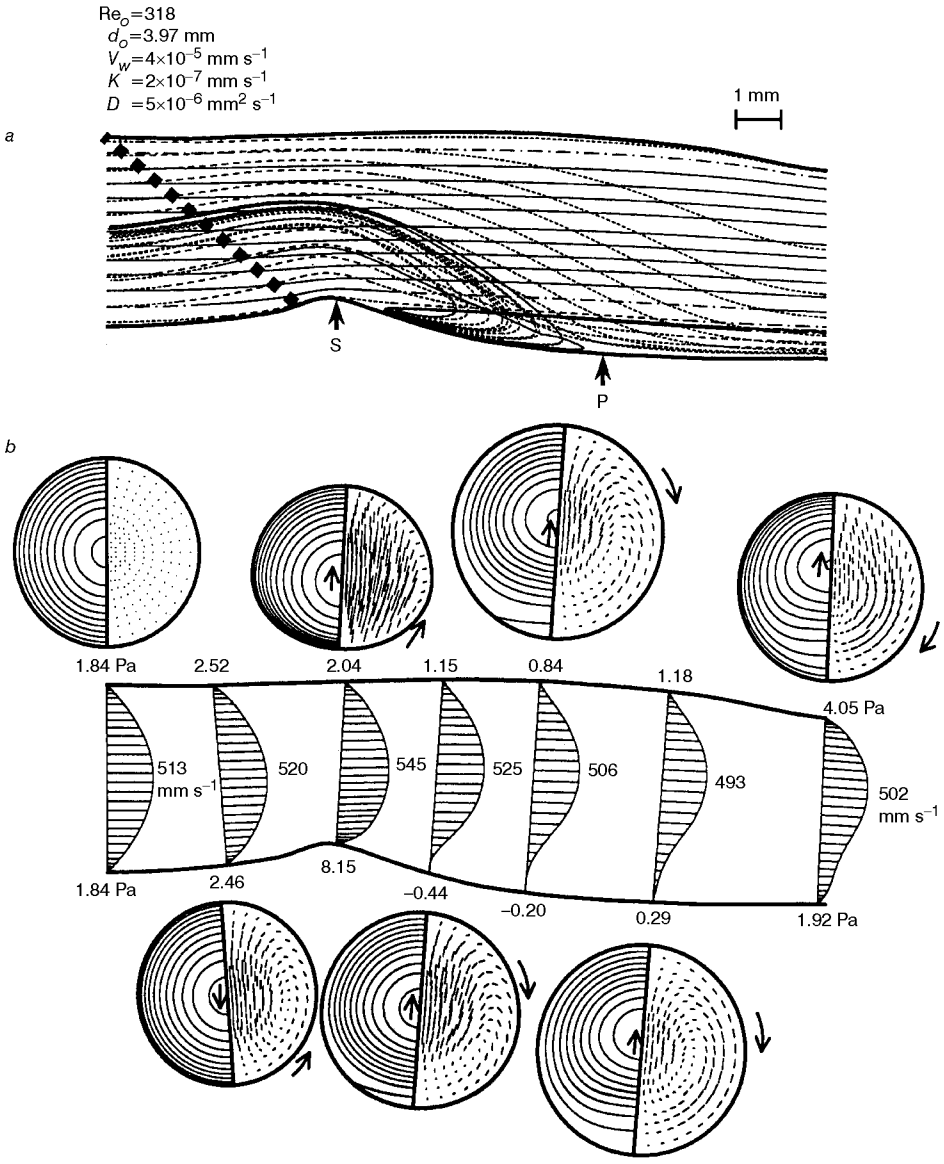

Fig. 3 *(a) Detailed flow pattern in anastomosed artery containing moderate stenosis at inflow Reynolds number $Re_o = 318$, obtained by tracing paths of fluid elements chosen to depict characteristics of flow in this vessel. Velocity range, mm s^{-1}: (····) 0–5; (- - -) 50–100; (- · -) 100–200; (——) >200. (b) Distributions of fluid velocity and wall shear stress in bisector plane. Vector plots of flow pattern and contour map of fluid axial velocity in cross-section of vessel are also shown respectively, in right and left halves of cross-section at each location where velocity distribution is shown. S and P indicate separation and stagnation points, respectively. Numbers outside vessel indicate values of wall shear stress evaluated at each location*

indicated by the broken lines, and wall shear stress was locally elevated on both the inferior and superior walls in the region of the anastomotic junction. However, no recirculation flow was formed distal to the anastomotic junction, and there was no region where wall shear stress was lower than that found in an undisturbed region proximal to the anastomotic junction. These characteristics of the flow in the anastomosed vessel without a stenosis were also qualitatively the same as those found experimentally.

3.2 *Distribution of surface concentration of LDLs*

Using the fluid velocities obtained for each computational model of the anastomosed artery, calculations of mass transport of LDLs were carried out, assuming that the water filtration velocity at the vessel wall $V_w = 4 \times 10^{-5}$ mm s^{-1} (TEDGUI *et al.*, 1984), the overall mass transfer coefficient of LDLs at the vessel wall $K = 2 \times 10^{-7}$ mm s^{-1}. BRATZLER *et al.*, 1977; TRUSKEY *et al.*, 1992) and the diffusivity of LDLs in blood $D = 5 \times 10^{-6}$ mm^2 s^{-1}.

Fig. 5 shows a contour map of LDL concentration at the luminal surface of the anastomosed artery containing a moderate stenosis. The velocity distributions for this vessel are shown in Fig. 3. In this Figure, the surface concentrations of LDLs C_w are normalised by the value at the inlet C_o, and their magnitudes are expressed by colours and contour lines, as shown in the upper and lower panels, respectively. A colour scale for the colour map is shown in the upper right corner of this Figure, and the contour lines in the lower panel are drawn at intervals of a 2.5% change in normalised concentration of LDLs. Owing to the difficulty often encountered in the calculation of mass transport of a substance with low diffusivity, which results in mass transport with a high Peclet number, the shapes of the colour map and the contour lines of the surface concentration of LDLs obtained were spiny, making the Figure ugly. However, it was found that owing to the semipermeable nature of the arterial wall, concentration polarisation of LDLs certainly occurred at the luminal surface of the blood vessel, creating some regions of high and low surface concentration of LDLs in the anastomosed artery, depending on the degree of flow disturbances caused by the presence of a

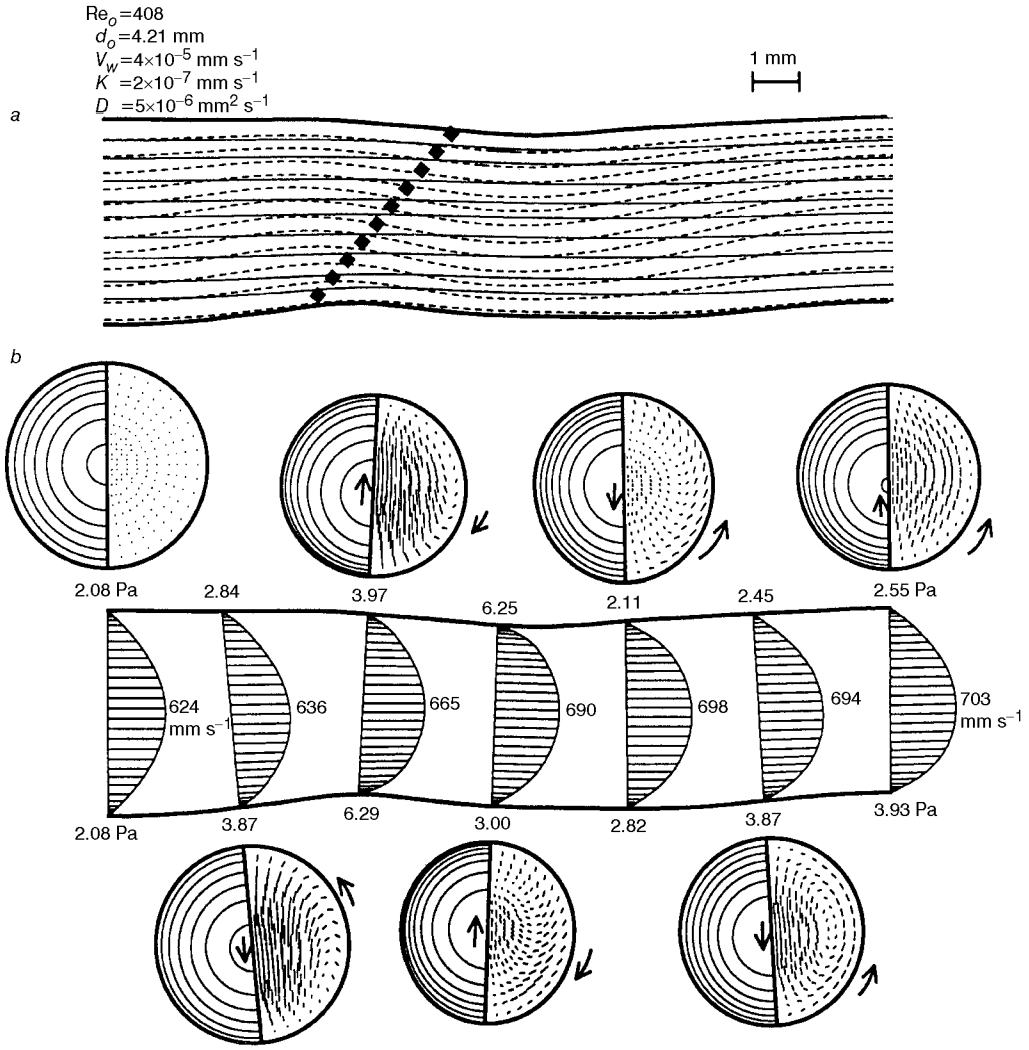

Fig. 4 *(a) Detailed flow pattern in anastomosed artery without stenosis at inflow Reynolds number $Re_o = 408$, obtained by tracing paths of fluid elements that were chosen to depict characteristics of flow in this vessel. Velocity range, mm s^{-1}: (····) 0–50; (- - -) 50–100; (- · -) 100–200; (——) >200. (b) Distributions of fluid velocity and wall shear stress in bisector plane. Vector plots of flow pattern and contour map of fluid axial velocity in cross-section of vessel are also shown, respectively, in right and left halves of cross-section at each location where velocity distribution is shown. Numbers outside vessel indicate values of wall shear stress evaluated at that location*

stenosis. As evident from this Figure, the surface concentration of LDLs was locally elevated by more than 10% in a restricted region distal to the stenosis, where a recirculation zone was formed, whereas, in other regions, it increased by only 5% or less. The highest value of C_w/C_o, which was found just downstream of the apex of the stenosis, was 1.19, and the location corresponded well to the site where intimal thickening developed preferentially.

Fig. 6 shows a contour map of the surface concentration of LDLs in the anastomosed artery containing no stenosis, in which no recirculation zone was formed. Velocity distributions for this vessel are shown in Fig. 4. It was found that the surface concentration of LDLs increased slightly (2.5% from the value at the inlet) in the region distal to the anastomotic junction, but there was no particular region where the surface concentration of LDLs was locally elevated in this vessel.

3.3 *Relationship between near-wall flow pattern, wall shear stress and surface concentration of LDLs in region of recirculation flow*

Fig. 7 shows a detailed near-wall flow pattern expressed with velocity vectors at locations 5 μm (corresponding to the size of one mesh) away from the vessel wall, a contour map of wall shear stress (Fig. 7*a*) and a contour map of the surface concentration of LDLs (Fig. 7b) in the anastomosed artery containing a moderate stenosis, as observed normal to the inferior wall distal to the apex of the stenosis where a recirculation zone was formed. The contour lines were drawn at intervals of a 0.1 Pa change in wall shear stress τ_w and a 2.5% change in normalised surface concentration of LDLs C_w/C_o.

As shown in the near-wall flow pattern, flow separation occurred not only at one point S in the bisector plane of the vessel just distal to the apex of the stenosis, but also along an arched line that extended from the point S to both sides of the bisector plane, and the fluid elements forming part of the thin-layered peripheral secondary flows, which came from the lateral walls in a paired structure, entered the region of separated flow from both sides. Then, some of the fluid elements that entered from points very close to both edges of the separation line changed their directions and travelled backwards towards the separation point S, and then they suddenly changed direction and were drawn along by the mainstream in and very close to the bisector plane of the vessel. Others that entered from points far from the edges of the separation line moved towards the bisector plane and encountered the fluid elements from the other side, and then just flowed straight down.

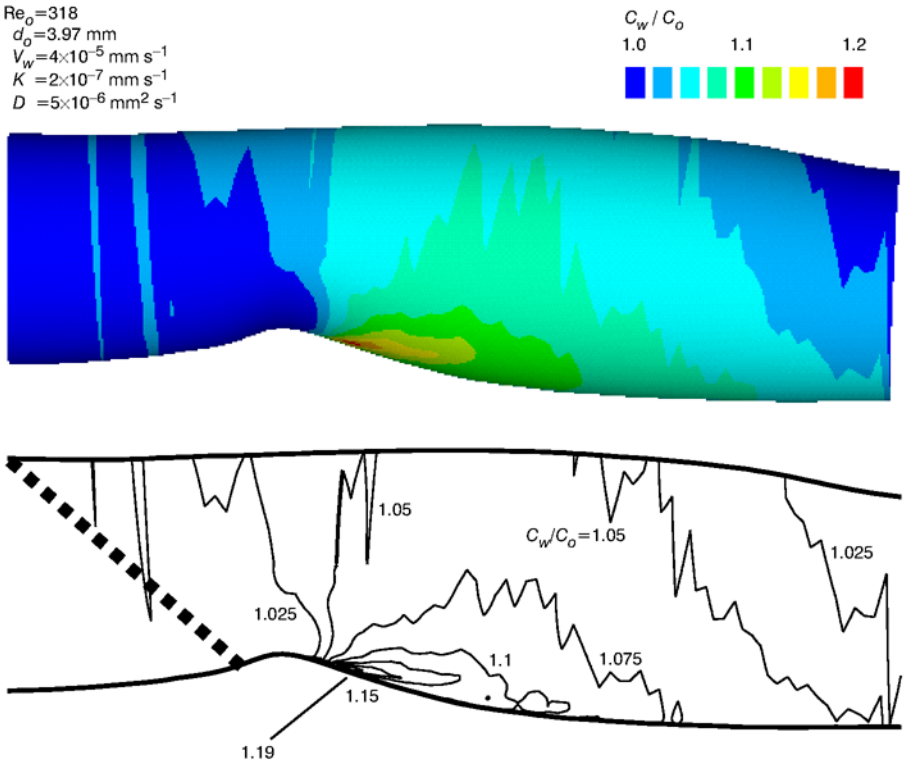

Fig. 5 *Contour map of LDL concentration at luminal surface of anastomosed artery containing moderate stenosis at $Re_o = 318$, as observed normal to bisector plane of vessel. Colour scale is shown in upper right. Contour lines were drawn at intervals of 2.5% change in normalised surface concentration of LDLs C_w/C_o*

In this way, a standing recirculation (adverse flow) zone, which occupied an elliptical area on the lower wall between the separation line and the stagnation point P, was formed just distal to the apex of the stenosis created at the site of an anastomotic junction, as shown in Fig. 7. In the recirculation zone, near-wall velocity of the fluid element was highest in the bisector plane, and it increased from zero at the stagnation point P, reaching a maximum at a location a little closer from the midpoint to the separation point S, and then decreased to zero at the separation point S. Therefore the region of very low wall shear stress was located at the periphery of the elliptical recirculation zone, where fluid elements in the vicinity of the vessel wall encountered the fluid elements from their opposite directions and formed stagnation points, as shown in the upper half of Fig. 7*a*.

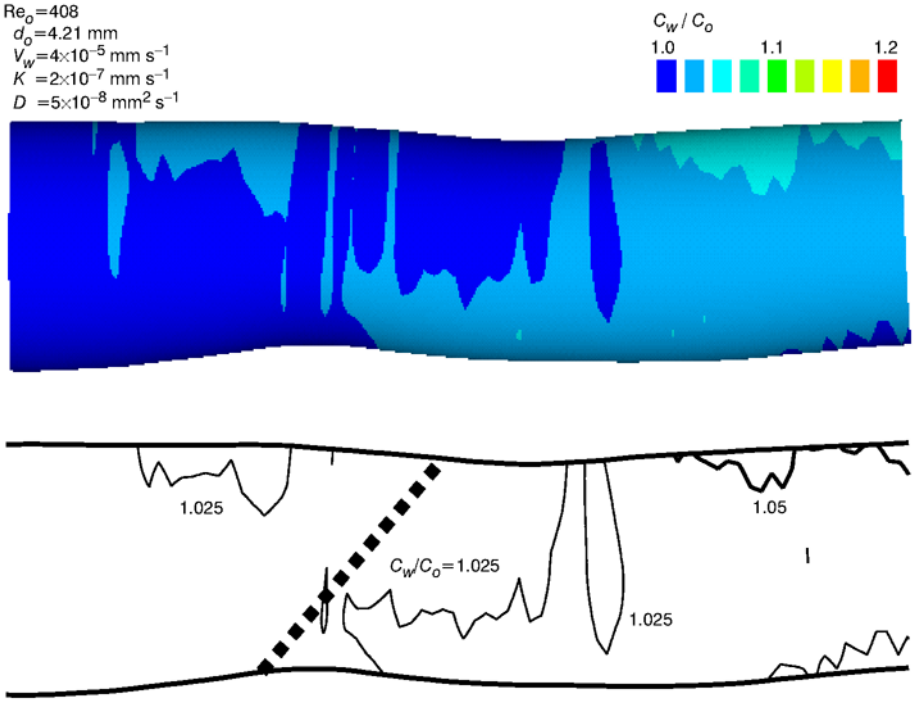

Fig. 6 *Contour map of LDL concentration at luminal surface of anastomosed artery without stenosis at $Re_o = 408$, as observed normal to bisector plane of vessel. Colour scale for colour map is shown in upper right. Contour lines were drawn at intervals of 2.5% change in normalised surface concentration of LDLs C_w/C_o*

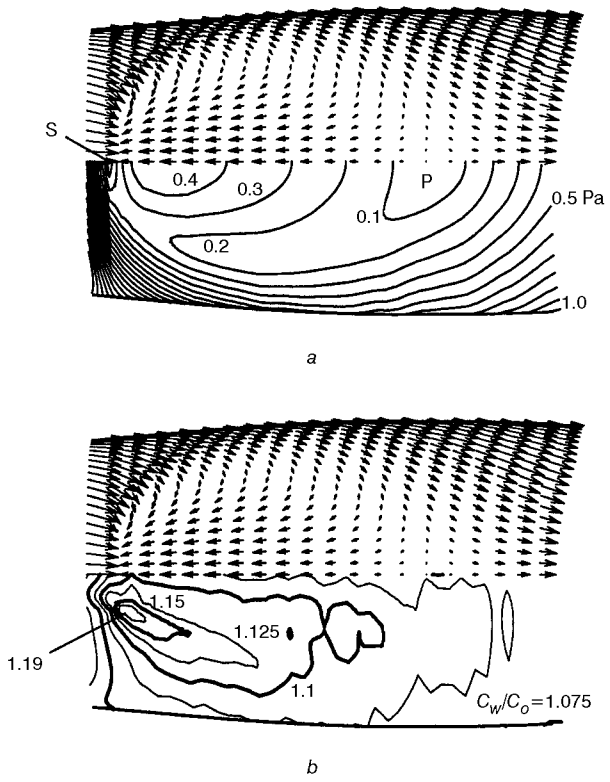

Fig. 7 *(a) Detailed near-wall flow pattern expressed with velocity vectors at locations 5 μm away from vessel wall, contour map of wall shear stress and contour map of surface concentration of LDLs at inferior wall distal to stenosis, where recirculation zone was formed (see Fig. 3) and surface concentration of LDLs was locally elevated (see Fig. 5)*

In the present case, there were four distinct regions where fluid velocity and wall shear stress were very low. Out of these, two were the regions that included the points of flow separation S and flow stagnation P, located in the bisector plane of the vessel. The other two regions were located close to the separation point S, but on both sides of the bisector plane just distal to the arched separation line. These two regions were the very spots where the fluid elements in the thin-layered peripheral secondary flows that came from the lateral wall encountered the fluid elements in the adverse flow and formed a stagnation point. The point of the highest surface concentration of LDLs was located within these two regions, as shown by a contour map in the lower half of Fig. 7*b*. The surface concentration of LDLs at these two stagnation points was approximately 20% higher than that at the entrance and the bulk flow.

3.4 *Effect of locally varying water filtration velocity on surface concentration of LDLs*

We have shown in this study that a local flow disturbance created by the presence of a stenosis in an anastomosed artery affects the transport of LDLs to the artery, resulting in the formation of regions of high and low LDL concentration at the luminal surface of the arterial wall. This concentration polarisation of LDLs is caused by the presence of a water filtration flow at the vessel wall. Hence, to find ways of reducing intimal thickening at the anastomotic junction, we tested the effect of water filtration velocity on LDL concentration at the luminal surface of the anastomosed artery, by locally varying the value of the water filtration velocity at the wall in the receding portion of the stenosis where blood flow was locally disturbed. Calculations were carried out for blood flowing at $Re_o = 318$ through the anastomosed artery containing a moderate stenosis. It was assumed that, as shown in Fig. 8, the water filtration velocity at the vessel wall varied only in the segment distal to the stenosis surrounded by broken lines, where a recirculation zone was formed. The values of the water filtration velocity at the wall proximal and distal to the segment were set to be $V_w = 4 \times 10^{-5}$ mm s^{-1}, and the value at the segment was varied in the three steps, namely, $\bar{V}_w = 8 \times 10^{-5}$, 4×10^{-5} and 4×10^{-6} mm s^{-1}.

Fig. 8 shows the distribution of LDL concentration at the luminal surface of the anastomosed artery. The regions of high and low LDL concentrations are expressed by red and blue respectively. As shown in Fig. 8*b*, it was found that the concentration polarisation of LDLs was augmented by increasing the water filtration velocity at the vessel wall, and the surface concentration of LDLs was elevated up to 30% from the value at the inlet at the receding portion of the stenosis by raising the water filtration velocity to a value two times higher than that in the proximal and distal segments of the anastomosed artery. In contrast to this, as shown in Fig. 8*c*, there was no area where the surface concentration of LDLs was locally elevated in the anastomosed artery when the water filtration velocity in the segment containing the anastomotic junction was decreased to a value one order lower than that in the proximal and distal segments. These results suggested that elevation of the surface concentration of LDLs at the receding portion of the stenosis, which was caused by a disturbance of blood flow, could be reduced by locally decreasing the water filtration velocity at the vessel wall.

4 Discussion

4.1 *Validity of the present calculations*

Using the same anastomosed arteries as those adopted in the present study to construct anatomically realistic models for computational analyses of blood flow and LDL transport, ISHIBASHI *et al.* (1995) have carried out flow studies and histological examinations of arterial walls. They showed that, in the case of the anastomosed artery with a stenosis shown in Fig. 1*a*, flow separation occurred around the apex of the stenosis, resulting in the formation of a region of slow recirculation flow with low wall shear stress distal to it. They also showed that a moderate intimal thickening occurred adjacent to the recirculation zone, with the point of maximum thickness located around the point of flow separation. In contrast to this, in the case of the anastomosed artery without a stenosis shown in Fig. 1*b*, neither formation of a recirculation zone nor development of an intimal thickening was observed. The difference in flow patterns between these two anastomosed arteries were well represented by our calculations, as shown in Figs 3 and 4. As we assumed in the calculation that the distribution of fluid velocity at the inlet of the artery was parabolic and the geometry of the vessel was symmetric with respect to the bisector plane of the vessel, the flow paths calculated for the artery with a moderate stenosis (Fig. 3) were slightly different from those obtained experimentally (Fig. 1*a*).

To be more specific, the recirculation zone obtained experimentally occupied a slightly wider area distal to the stenosis than that obtained by our calculation. Therefore we may be underestimating the effect of local flow disturbance on the occurrence of intimal thickening and LDL transport in the anastomosed artery. However, the results obtained by our computational analyses are consistent with the experimental finding that there was a strong positive correlation between the preferred sites of intimal thickening and the regions of slow recirculation flows with low wall shear stresses in end-to-end anastomosed arteries.

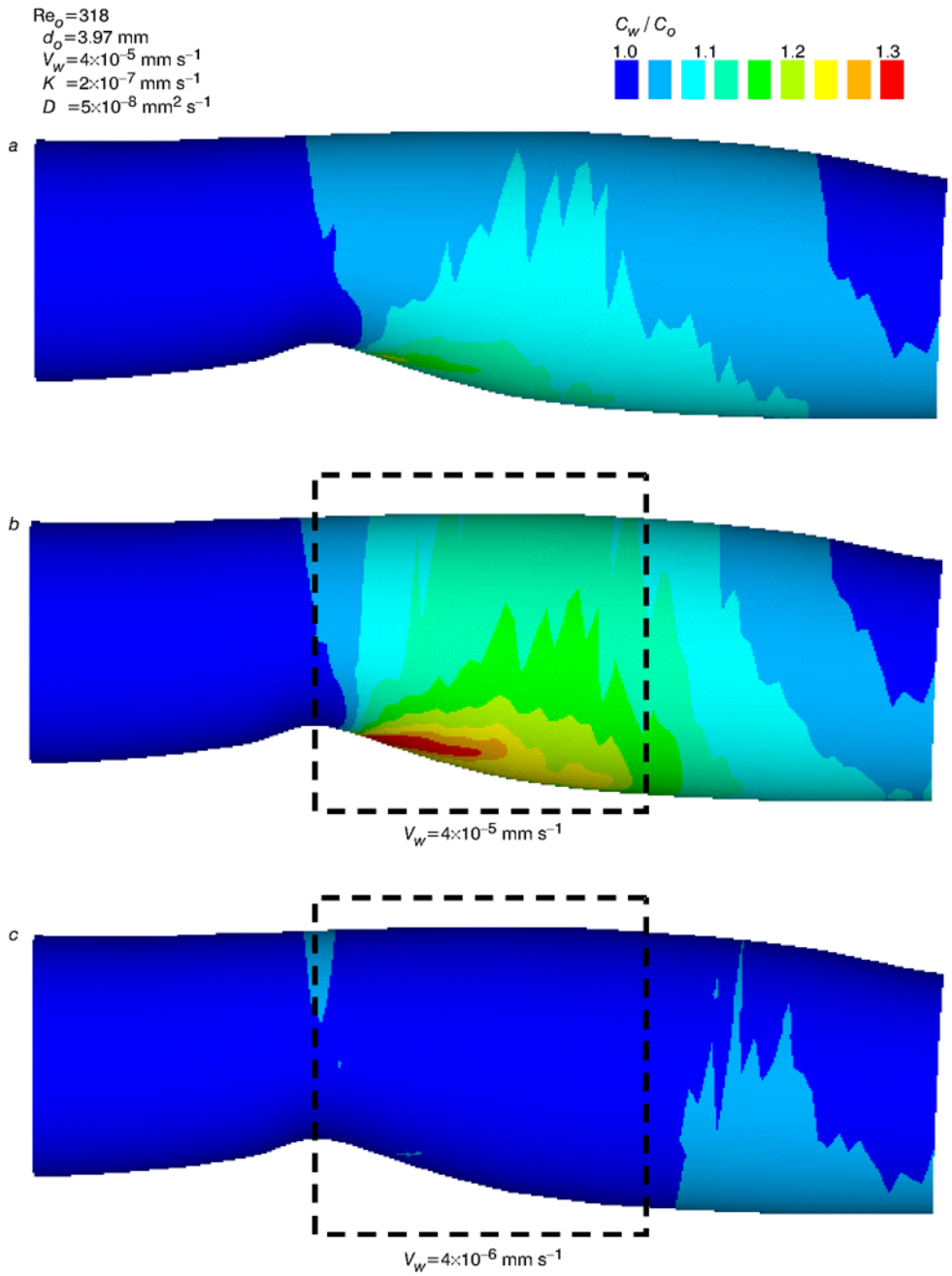

Fig. 8 *Effect of water filtration velocity at vessel wall on distribution of LDL concentration at luminal surface of anastomosed artery containing moderate stenosis. Note that locally elevated surface concentration of LDLs distal to apex of stenosis was further increased or decreased by locally increasing and decreasing water filtration velocity*

As the diffusivity of LDLs used for the calculations of LDL transport was very small, the Peclet number became extremely large, making it difficult to solve the governing equation numerically. To overcome this, the solution domain for LDL transport was limited to a region near the vessel wall, where fluid velocity was low, because the concentration of LDLs changes only in the vicinity of the wall (WADA and KARINO, 1999; 2002a). Furthermore, we adopted smaller-sized elements for the calculation of LDL transport by dividing the elements used for the calculation of blood flow into two sub-elements in the radial direction. Concerning the convergence of the solution with the element size, we have examined this by carrying out calculations of LDL transport using various element sizes. As a result, it was confirmed that the value of the maximum surface concentration of LDLs converges as the number of re-division of each element in the radial direction increases, and an adequate value was obtained in the present calculation. Although numerical fluctuation remained in the contour map of LDL surface concentration shown in Figs 5 and 6, the value of LDL concentration falls into a physical range ($0.996 < C/C_o < 1.19$). Therefore we considered that the numerical solution for LDL concentration obtained by our calculation was accurate enough and acceptable.

4.2 *Relationship between intimal thickening and surface concentration of LDLs*

Our new finding in the present study was that, owing to the semipermeable nature of the vessel wall, concentration polarisation of LDLs occurred at the luminal surface of the anastomosed artery, and the surface concentration of LDLs was locally elevated at a site where flow was locally disturbed and wall shear stress was relatively low. Moreover, the site of high LDL concentration corresponded well with the site where

intimal thickening was observed (ISHIBASHI *et al.*, 1995). In contrast to this, no significant elevation of surface concentration of LDLs occurred in the anastomosed artery in which no stenosis was formed and no intimal thickening was observed. These results suggested that the number of LDLs accumulated on the luminal surface of the arterial wall (surface concentration of LDLs) was directly reflected in the number of LDLs taken up by the arterial wall, leading to thickening of the vessel wall. With respect to this, there have been several articles that reported that elevation of the lipoprotein level in blood promoted the uptake and internalisation of LDLs (VASILE *et al.*, 1983) and accumulation of cholesterol and its ester within the intima of arteries (ROSS and HARKER, 1976; HOFF and WAGNER, 1986), leading to the development of atherosclerotic lesions and intimal hyperplasia both in humans and experimental animals (KLYACHKIN *et al.*, 1993; STARY *et al.*, 1994; BAUMANN *et al.*, 1994; HUNNINGHAKE, 1998; CAMPEAU, 2000). What we have shown in our present work is that local flow dynamics affects, not only the distribution of wall shear stress, but also the transport of LDLs from flowing blood to an arterial wall, creating preferred sites of intimal thickening in anastomosed arteries. The fact that the surface concentration of LDLs is still elevated at the very site where intimal thickening has already occurred suggests that there is a possibility that thickening of the intima further progresses at this site.

4.3 *Our viewpoint on the role of haemodynamics in the localisation of vascular diseases*

It has been considered that localised pathogenesis and development of anastomotic intimal hyperplasia and atherosclerosis occur as summations of various biological responses to mechanical stimulations given to the endothelium of arterial walls by wall shear stress. Thus most researchers investigating the mechanisms of the localisation of these diseases have concentrated their efforts on finding the value of wall shear stress in various arteries and its spatial and temporal variations (ZARINS *et al.*, 1983; KU *et al.*, 1985; SOTTIURAI *et al.*, 1989; ASAKURA and KARINO, 1990; BASSIOUNY *et al.*, 1992; PEDERSEN *et al.*, 1999; KLEINSTREUER *et al.*, 2001).

Certainly, the results of the experimental study by ISHIBASHI *et al.*, (1995) and our calculations showed that intimal thickening occurred at sites of low wall shear stress in the anastomosed artery with a stenosis. However, the region of low wall shear stress, which extended from the point of flow separation to the stagnation point covering the whole area occupied by recirculation flows, contained a wide area where no intimal thickening occurred (Fig. 7). Therefore it was suggested that there are several factors relating to local flow dynamics that distinguish the particular region of low wall shear stress from other regions and that lead to localised genesis and development of intimal thickening.

As shown in Fig. 7, in the recirculation zone, the surface concentration of LDLs was significantly elevated only at the receding portion of the stenosis close to the point of flow separation, where intimal thickening developed. Despite the low wall shear stress, the surface concentration of LDLs was not elevated as much around the stagnation point in the recirculation zone. Therefore it was considered that the difference in surface concentration of LDLs reflected the difference in local flow pattern that created the region of low wall shear stress.

Our previous studies on LDL transport through a straight artery (WADA and KARINO, 1999) showed that the surface concentration of LDLs increases with decreasing flow rate, hence wall shear stress, and increasing the distance from the entrance of the artery, indicating that the concentration polarisation of LDLs is augmented by elongating the period during which LDL molecules travel along the vessel wall in contact with the wall, as water content in blood decreases by the presence of a filtration flow at the vessel wall.

If we consider the same mechanism for the case of the anastomosed artery with a moderate stenosis used in the present study, it is expected that the highest surface concentration of LDLs appears, not at the point of flow separation, as the concentration boundary layer is destroyed at that point, but at sites somewhere in the recirculation zone, where fluid elements and LDL molecules arrive after travelling a long distance along the anterior and posterior walls and stay for a long time before leaving the region of separated flow by being drawn along by the fast mainflow. This is exactly what we found in our present study (see Figs 3 and 7).

Therefore it was confirmed that the surface concentration of LDLs is determined, not only by the value of wall shear stress at a location, but by near-wall flow patterns that determine the paths and the velocities of fluid elements and LDL molecules taken to reach a particular site and the duration of their interactions and contact with the vessel wall, which could be important for the uptake of LDLs by endothelial cells. This is our novel viewpoint on local flow dynamics creating a low shear region based on mass transport, and it consistently explains the experimental finding that there exists a strong and positive correlation between the preferred sites of intimal thickening and the regions of slow recirculation flows with low wall shear stresses in the end-to-end anastomosed artery.

4.4 *Concentration polarisation of LDLs under in vivo conditions*

It should be noted that our calculations of LDL transport in flowing blood were carried out under the assumption that the flow was steady and the permeability of the endothelium to water and LDL was uniform in the artery. Under the *in vivo* condition, the concentration polarisation of LDLs would be impaired by flow disturbances created by the pulsatility of the blood flow, especially in the region where a recirculation zone forms and vanishes periodically. It would also be affected by a regional difference in permeability of the endothelium (CHUANG, *et al.*, 1990), especially where there are leaky spots (WEINBAUM *et al.*, 1985) and by its dependency on wall shear stress (JO *et al.*, 1991; FRIEDMAN *et al.*, 2000).

Regarding the effect of the pulsatility of the flow on the concentration polarisation of LDLs, we previously carried out calculations of surface concentration of LDLs in an artery with a multiple bend by varying the Reynolds number periodically (WADA and KARINO, 2002*a*). We found that, although the degree of concentration polarisation was diminished by the pulsatility of the flow, the location of the specific region of high surface concentration of LDLs remained almost the same as that found under the condition of a steady flow.

Regarding the effect of the regional difference in permeability of the endothelium to water and LDLs, we calculated the distribution of LDL concentration at the bumpy luminal surface of the endothelium, where filtration of water is confined to junctions of endothelial cells, and confirmed that the concentration polarisation of LDLs certainly occurs even in this case (WADA and KARINO, 2002*b*). It has also been shown that the intima of an arterial wall, where atherosclerotic changes and intimal thickening occurred or tend to occur, is easily stained with dyes such as Evans blue (FRY, 1977), indicating that the permeability of the vessel wall to plasma proteins is increased there. However, the permeability of the endothelium to LDLs must be much smaller than that to water, even at such a leaky spot, as the molecular size of LDL is much larger than that of water. Therefore we considered that the concentration of

polarization of LDLs occurs even *in vivo* at such sites, although the degree of concentration polarisation will be affected by flow disturbances created by the pulsatile flow prevailing there.

4.5 *Application of the results obtained to a clinical problem*

As an application of the results obtained by the present computational studies to a clinical problem, we showed that, by reducing the water filtration velocity at the vessel wall around the anastomotic junction, including the preferred sites of intimal thickening, we can lower the surface concentration of LDLs there. This suggests that the development of anastomotic intimal hyperplasia could be prevented by lowering the permeability of the endothelium by either topically applying a drug to the vessel wall or externally coating the portion of the vessel with a water-impermeable material. In connection with this, there have been several interesting reports that, in bypass grafting, interposition of a short segment of a vein (a vein cuff) between an expanded polytetrafluoroethylene (ePTFE) graft and an artery at a distal anastomotic site diminished intimal hyperplasia and improved long-term patency rate (MILLER *et al.*, 1984; TYRRELL and WOLFE, 1991; TAYLOR *et al.*, 1992).

It is very likely that, as the permeability of the wall of a vein to plasma is much lower than that of the ePTFE graft, even after its implantation in the arterial system, the presence of the interposed vein cuff reduces the degree of concentration polarisation of LDLs at the luminal surface of both the graft and host artery in the region of the anastomotic junction, resulting in a lower uptake of LDLs by the endothelial cells there. Reduction of flow disturbances in the anastomosed vessel, by attenuation of the compliance mismatch between the graft and the artery through adaptive changes of the geometric structure of the walls of both the interposed vein and the host artery at the anastomotic junction, would help reduce the regions where concentration polarisation of LDLs occurs.

Although there is no evidence directly to support our speculation, it has been shown that an increase in the permeability of a vessel wall to plasma leads to the development of intimal thickening (MII *et al.*, 1990), even if the luminal surface of the vessel is completely covered with endothelial cells (WADA *et al.*, 2001*a*). Judging from the above result, it is also foreseeable that, in contrast to the above case, a decrease in the water permeability of a vessel wall leads to the mitigation of intimal hyperplasia. To confirm our prediction, it is necessary further to investigate experimentally the effects of the water permeability of a vessel wall on the uptake of LDLs by endothelial cells and the development of intimal hyperplasia.

Acknowledgments—This work was partially supported by the Grant-in-Aid for Scientific Research (B), number 13480284, provided by the Ministry of Education, Science, Sports & Culture of Japan.

References

ASAKURA, T., and KARINO, T. (1990): 'Flow patterns and spatial distribution of atherosclerotic lesions in human coronary arteries', *Circ. Res.*, **66**, pp. 1045–1066

BASSIOUNY, H. S., WHITE, S., GLAGOV, S., CHOI, E., GIDDENS, D. P., and ZARINS, C. K. (1992): 'Anastomotic intimal hyperplasia: mechanical injury or flow induced', *J. Vasc. Surg.*, **15**, pp. 708–717

BAUMANN, D. S., DOBLAS, M., DAUGHERTY, A., SICARD, G., and SCHONFELD, G. (1994): 'The role of cholesterol accumulation in prosthetic vascular graft anastomotic intimal hyperplasia', *J. Vasc. Surg.*, **19**, pp. 435–445

BRATZLER, B. L., CHISOLM, G. M., COLTON, C. K., SMITH, K. A., and LEES, R. S. (1977): 'The distribution of labeled low-density lipoproteins across the rabbit thoracic *in vivo*', *Atherosclerosis*, **28**, pp. 289–307

BROOKS, A. N., and HUGHES, T. J. R. (1982): 'Streamline upwind/Petrov–Galerkin formulations for convection dominated flows with particular emphasis on the incompressible Navier–Stokes equations', *Comput. Methods Appl. Mech. Eng.*, **32**, pp. 199–259

CAMPEAU, L. (2000): 'Lipid lowering and coronary bypass graft surgery', *Curr. Opin. Cardiol.*, **15**, pp. 395–399

CHUANG, P. T., CHENG, H. J., LIN, S. J., JAN, K. M., LEE, M. M., and CHIEN, S. (1990): 'Macromolecular transport across arterial and venous endothelium in rats. Studies with Evans blue-albumin and horseradish peroxidase', *Arteriosclerosis*, **10**, pp. 188–197

CLOWES, A. W., GOWN, A. M., HANSON, S. R., and REIDY, M. A. (1985): 'Mechanisms of arterial graft failure. 1. Role of cellular proliferation in early healing of PTFE prostheses', *Am. J. Pathol.*, **118**, pp. 43–54

DENG, X., MAROIS, Y., HOW, T., MERHI, Y., KING, M., GUIDOIN, R., and KARINO, T. (1995): 'Luminal surface concentration of lipoprotein (LDL) and its effect on the wall uptake of cholesterol by canine carotid arteries', *J. Vasc. Surg.*, **21**, pp. 135–145, and **22**, pp. 9A and 648

FRIEDMAN, M. H., HENDERSON, J. M., AUKERMAN, J. A., and CLINGAN, P. A. (2000): 'Effect of periodic alterations in shear on vascular macromolecular uptake', *Biorheology*, **37**, pp. 265–277

FRY, D. L. (1977): 'Aortic Evans blue dye accumulation: its measurement and interpretation', *Am. J. Physiol.*, **232**, (*Heart Circ. Physiol.*, **1**), pp. H204–H222

GUIDOIN, R., COUTURE, J., ASSAYED, F., and GOSSELIN, C. (1988): 'New frontiers of vascular grafting', *Int. Surg.*, **73**, pp. 241–249

HOFF, H. F., and WAGNER, W. D. (1986): 'Plasma low density lipoprotein accumulation in aortas of hypercholesterolemic swine correlates with modifications in aortic glycosaminoglycan composition', *Atherosclerosis*, **61**, pp. 231–236

HUNNINGHAKE, D. B. (1998): 'Is aggressive cholesterol control justified? Review of the post-coronary artery bypass graft trial', *Am. J. Cardiol.*, **82**, pp. 45T–48T

IMPARATO, A. M., BRACCO, A., KIM, G. E., and ZEFF, R. (1972): 'Intimal and neointimal fibrous proliferation causing failure of arterial reconstructions', *Surgery*, **72**, pp. 1007–1017

ISHIBASHI, H., SUNAMURA, M., and KARINO, T. (1995): 'Flow patterns and preferred sites of intimal thickening in end-to-end anastomosed vessels', *Surgery*, **117**, pp. 409–420

JO, H., DULL, R. O., HOLLIS, T. M., and TARBELL, J. M. (1991): 'Endothelial albumin permeability is shear dependent, time dependent, and reversible', *Am. J. Physiol.*, **260**, pp. H1992–H1996

KARINO, T., and MOTOMIYA, M. (1983): 'Flow visualization in isolated transparent natural blood vessel', *Biorheology*, **20**, pp. 119–127

KLEINSTREUER, C., HYUN, S., BUCHANAN, J. R. Jr., LONGEST, P. W., ARCHIE, J. P. Jr., and TRUSKEY, G. A. (2001): 'Hemodynamic parameters and early intimal thickening in branching blood vessels', *Crit. Rev. Biomed. Eng.*, **29**, pp. 1–64

KLYACHKIN, M. L., DAVIES, M. G., SVENDSEN, E., KIM, J. H., MASSEY, M. F., BARBER, L., MCCANN, R. L., and HAGEN, P. O. (1993): 'Hypercholesterolemia and experimental vein grafts: accelerated development of intimal hyperplasia and an increase in abnormal vasomotor function', *J. Surg. Res.*, **54**, pp. 451–468

KU, D. N., GIDDENS, D. P., ZARINS, C. K., and GLAGOV, S. (1985): 'Pulsatile flow and atherosclerosis in the human carotid bifurcation: positive correlation between plaque location and low oscillating shear stress', *Arteriosclerosis*, **5**, pp. 293–302

MII, S., OKADOME, K., ONOHARA, T., YAMAMURA, S., and SUGIMACHI, K. (1990): 'Intimal thickening and permeability of arterial autogenous vein graft in a canine poor-runoff model: transmission electron microscopic evidence', *Surgery*, **108**, pp. 81–89

MILLER, J. H., FOREMAN, R. K., FERGUSON, L., and FARIS, I. (1984): 'Interposition vein cuff for anastomosis of prosthesis to small artery', *Aust. N. Z. J. Surg.*, **54**, pp. 283–285

NAIKI, T., SUGIYAMA, H., Tashiro, R., and KARINO, T. (1999): 'Flow-dependent concentration polarization of plasma proteins at the luminal surface of a cultured endothelial cell monolayer', *Biorheology*, **36**, pp. 225–241

PEDERSEN, E. M., QYRE, S., AGERBAEK, M., KRISTENSEN, I. B., RINGGAARD, S., BOESIGER, P., and Paaske, W. P. (1999): 'Distribution of early atherosclerotic lesions in the human abdominal aorta correlates with wall shear stresses measured in vivo', *Eur. J. Vasc. Endovasc. Surg.*, **18**, pp. 328–333

ROSS, R., and HARKER, L. (1976): 'Hyperlipidemia and atherosclerosis: chronic hyperlipidemia initiates and maintains lesions by endothelial cell desquamation and lipid accumulation', *Science*, **193**, pp. 1094–1100

SOTTIURAI, V. S., YAO, J. S., BATSON, R. C., SUE, S. L., JONES, R., and NAKAMURA, Y. A. (1989): 'Distal anastomotic intimal hyperplasia: histopathologic character and biogenesis', *Ann. Vasc. Surg.*, **3**, pp. 26–33

STARY, H. C., CHANDLER, A. B., GLAGOV, S., GUYTON, J. R., INSULL, W. Jr., ROSENFELD, M. E., SCHAFFER, A., SCHWARTZ, C. J., WAGNER, W. D., and WISSLER, R. W. (1994): 'A definition of initial, fatty streak, and intermediate lesions of atherosclerosis: a report from the committee on vascular lesions of the council on arteriosclerosis', *Arterioscler. Thromb.*, **14**, pp. 840–856

TAYLOR, R. S., LOH, A., MCFARLAND, R. J., COX, M., and CHESTER, J. F. (1992): 'Improved technique for polytetrafluoroethylene bypass grafting: long-term results using anastomotic vein patches', *Br. J. Surg.*, **79**, pp. 348–354

TEDGUI, A., and LEVER, M. J. (1984): 'Filtration through damaged and undamaged rabbit thoracic aorta', *Am. J. Physiol.*, **247** (*Heart Circ. Physiol.*, **16**), pp. H784–H791

TRUSKEY, G. A., ROBERTS, W. L., HERRMANN, R. A., and MALINAUSKAS, R. A. (1992): 'Measurement of endothelial permeability to ^{125}I-low density lipoproteins in rabbit arteries by use of *en face* preparations', *Circ. Res.*, **71**, pp. 883–897

TYRRELL, M. R., and WOLFE, J. H. (1991): 'New prosthetic venous collar anastomotic technique: combining the best of other procedures', *Br. J. Surg.*, **78**, pp. 1016–1017

VASILE, K., SIMIONESCU, M., and SIMIONESCU, N. (1983): 'Visualization of the binding, endocytosis, and transcytosis of low-density lipoprotein in the arterial endothelium *in situ*', *J. Cell. Biol.*, **96**, pp. 1677–1689

WADA, S., and KARINO, T. (1999): 'Theoretical study on flow-dependent concentration polarization of low density lipoproteins at the luminal surface of a straight artery', *Biorheology*, **36**, pp. 207–223

WADA, S., and KARINO, T. (2002*a*): 'Theoretical prediction of LDL concentration at the luminal surface of an artery with a multiple bend', *Ann. Biomed. Eng.*, **30**, pp. 778–791

WADA, S., and KARINO, T. (2002*b*): 'Prediction of LDL concentration at the luminal surface of a vascular endothelium', *Biorheology*, **39**, pp. 331–336

WADA, S., KAICHI, M., and KARINO, T. (2001*a*): 'Changes in water filtration velocity and wall structure of the rabbit common carotid artery after removal of the adventitia', *JSME Int. J.*, **C44**, pp. 996–1004

WADA, S., KOUJIYA, M., and KARINO, T. (2001*b*): 'The effect of creating a moderate stenosis on the localization of intimal thickening in the common carotid artery of the rabbit fed on a cholesterol-rich diet', *JSME Int. J.*, **C44**, pp. 1021–1030

WEINBAUM, S., TZEGHAI, G., GANATOS, P., PFEFFER, R., and CHIEN, S. (1985): 'Effect of cell turnover and leaky junctions on arterial macromolecular transport', *Am. J. Physiol.*, **248**, pp. H945–H960

ZARINS, C. K., GIDDENS, D. P., BHARADVAJ, B. K., SOTTIURAI, V. S., MABON, R. F., and GLAGOV, S. (1983): 'Carotid bifurcation atherosclerosis: quantitative correlation of plaque localization with flow velocity profiles and wall shear stress', *Circ. Res.*, **53**, pp. 502–514

Author's biography

MAKOTO KOUJIYA was born in Wakkanai, Hokkaido Prefecture, Japan in 1970. He graduated from Faculty of Science, Tokyo University of Science in 1988, and received MEng degree in System Engineering from Hokkaido University in 2000. Presently, he is engaged in the development of an artificial heart pump at the R&D Center of Nikkiso Co., Ltd., Shizuoka, Japan.